J. Environ. Nanotechnol.
Volume 7, No.2 (2018) pp. 31-35
ISSN (Print): 2279-0748
ISSN (Online): 2319-5541
doi:10.13074/jent.2018.06.182306

Studies on $La_2In_{2-x}Al_2O_9$ Oxide Ion Conductors

N. Kalaivani, M.Rajasekhar*

Department of chemistry, Government Arts College, Dharmapuri, TN, India.

Received: 28.12.2017 *Accepted: 12.03.2018*

Abstract

$La_2In_{2-x}Al_2O_9$($0 \leq x \leq 0.5$) oxide ion conductor is synthesized with $La(NO_3)_3$, $In(NO_3)_3$, $Al(No_3)_3$and aspartic acid (fuel) by assisted combustion method, which is heating at 550˚C for 6 hours. X-ray diffraction analysis indicates that the orthorhombic structure of $La_2In_{2-x}Al_2O_9$. Scanning electron microscopy is used to identify the surface morphology. The particle size of the synthesized product is measured by the Scherrer equation and transmission electron microscope, its size 30 nm. The influence of the Al for Indium in $La_2In_{2-x}Al_2O_9$ of the phase transition has investigated by XRD studies. The formation of $La_2In_{2-x}Al_2O_9$ is confirmed by FTIR studies. The Arrhenius plot shows the ionic conductivity of $La_2In_{2-x}Al_2O_9$ on the variation of temperature. This result indicates that assisted combustion method is a promising method to prepare nanocrystalline $La_2In_{2-x}Al_2O_9$ oxide ion conductor for the solid oxide fuel cell.

Keywords: *Ionic conductivity; Scanning Electron Microscopy; Transmission Electron Microscope; Thermal Analysis; X-ray diffraction.*

1. INTRODUCTION

A fuel cell is a gadget that changes from chemical energy to electrical energy. The energy component is comprised of a cathode and anode isolated by an oxide particle conductor (electrolytes). The electrolyte with high oxygen conductivity is a key segment, and extensive variety of potential applications which including the electrolyte as oxygen sensors in strong oxide fuel cells and going is about as an oxygen-porous film in reactant frameworks (Jain et al. 1981; Lopez et al. 1997; Rajasekhar and Kalaivani, 2017).

A solid oxide fuel cell is a high working temperature fuel cell. They are absolutely imperativeness change tool that uses an oxide ion – coordinating solid electrolyte joined with ceramic cathodes. The standard purposes of the fuel cell are high capability, whole deal quality, fuel flexibility, low radiation, consolidating versatility in cell and arrangement, ease, creating methods and fuel plant assessment. The high working temperature between 500-1000 ˚C. They are profitable in far-reaching applications for aide power units, vehicles, stationary fuel age with yields from 100 W to 2 MW and tremendous scale industrial stations. The exorbitant catalysts are totally avoided, for instance, Platinum and Ruthenium etc. Solid Oxide Fuel Cell doesn't allow exorbitant metal oxides and metals as catalysts instead of the expensive and searcely open platinum driving forces. The high working temperatures organize the use of hydrocarbon fills without requiring an outside reformer to convey hydrogen fuel.

2. EXPERIMENTAL STUDIES & CHARACTERIZATION PROCESSES

The nano-crystalline $La_2In_{2-x}Al_2O_9$ (x = 0, 0.5, 1.0 and 1.5) powders were synthesized by assisted combustion method. In this method, a stoichiometric amount of $La(NO_3)_3$, $In(NO_3)_3$, $Al(NO_3)_3$ and aspartic acid were taken and made into homogeneous solutions by using double distilled water. All of the reagents in requisite stoichiometric amounts of the starting materials were dissolved in the double-distilled deionized water and in order to obtain a homogeneous solution. This solution was kept at constant heating at 80 ˚C to obtain the foamy powders of $La_2In_{2-x}Al_2O_9$, and the foamy powder was carried out in a muffle furnace at 550 ˚C for six hours. The oxidizing valency (O) of $La(NO_3)_3$ is –15, $Al(NO_3)$ is 6, $In(NO_3)_3$ is -15, and the reducing valency (F) of aspartic acid is +15. Hence the required amount of aspartic acid was

M. Rajasekhar
email: kalaikanishka2010@gmail.com

calculated for $Nd_2Mo_{1.5}In_{0.5}O_9$ as (2 ×-15) + (1.5 × 6) + (0.5 ×-15) + 15n = 0: n = 3.5 M

3. PHYSICAL CHARACTERIZATION

X-beam district is a piece of electromagnetic range going between 0.1 to 100 Å (identical to an energy of 0.1 – 100 KeV). The breaking of X-beams into dull and brilliant groups caused by the obstruction of one player in the bar with another when the beam is avoided by an obscure question with going with variety in the fuel of X - beams in various are ways is called X-beam diffraction. X - beam diffraction technique [Cullity, 1978; Sundar Manoharan and Kashinath C. Patil, 1992) is a standout amongst the most critical apparatuses for deciding nuclear courses of action in issues.

Filtering electron microscopy is utilized in the investigation of the surface geology of strong material. Filtering electron magnifying lens allows a profundity of the field for more than optical or transmission electron microscopy. The determination of the examining electron magnifying instrument is around 3nm, roughly two requests of size more noteworthy than the optical magnifying instrument. Along these lines, the SEM overcomes any issue between these two systems (Kostogloudis et al. 1997).

The size, shape and plan of the particles make up the example and also their relationship to each other on the size of nuclear breadths. The morphology and the ion size of the blended items were dissected by JOEL transmission magnifying instrument (Model: 1200 EX). The blended example was broke down with FTIR spectrometry, which is a district of around 4000 – 400cm^{-1}.

The heat deterioration of the polymeric forerunners was portrayed by Perkin-Elmer TG /DTA heat examination (Model; Pyris Diamond). The TGA is a procedure that depends on measuring the change in physical and substance properties of an example as an element of temperature (with steady heating rate) or as a component of time (with consistent temperature). It is overwhelmingly utilized for deciding the highlights of material that show either mass misfortune or increase because of disintegration, oxidation or loss of volatiles. Differential heat examination is a method in which the temperature of an example is contrasted and that of an inactive reference material amid the customized change of temperature.

A four-point test is put on a level surface of a strong example which can be approximated as semi-endless. An immediate current is gone through the sample between the external tests, and the subsequent potential distinction is measured between the entomb tests. The resistivity is figured from the present, and potential esteems and factors fitting to the geometry resistivity.

$$\rho = \frac{V}{I} 2\pi S \quad \text{(Ohm .cm)}$$

Where V –potential difference, I –current, S –probe spacing.

4.1 Analysis of Crystal Structure

The XRD patterns of the $La_2In_{2-x}Al_xO_9$ powders calcined at 550 ˚C for 6 hours are illustrated in Fig 4.1. X-ray diffraction information was utilized to ascertain crystallite size and its structure. Every one of the specimens demonstrated that solitary stage materials and the example recorded on the fundamental orthorhombic structure. The information reasoned that the cross-section volume expanded with expanding Indium content x. This outcome firmly proposed that helped ignition technique much lower calcination energy with shorter time length than strong state response strategy and different strategies. The normal crystallite size of $La_2In_{2-x}Al_xO_9$ nanopowder is at various compositions. The particle size measured from XRD data. The littler normal crystallite measure (nano ion) has been accomplished by utilizing helped ignition strategy contrasted with the ordinary strong state response technique and different strategies. The variety of the cross-section parameters of $La_2In_{2-x}Al_xO_9$ with Indium (In) content is shown in Fig 1 as the amount of Indium is increased with a decrease in the lattice parameter.

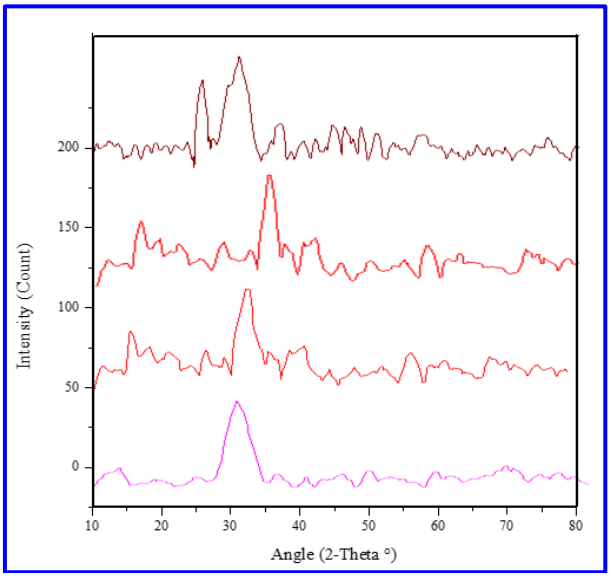

Fig. 4.1: X-ray diffraction pattern of $La_2In_{2-x}Al_xO_9$

4.2 Thermal Analysis (TGA/DTA)

$La_2In_{1.5}Al_{0.5}O_9$ nanocrystalline powder has been studied with thermogravimetric analysis (TGA) in the air is shown in Fig 4.2. In the TGA pattern, the $La_2In_{1.5}Al_{0.5}O_9$ sample showed a weight loss of about 0.048 mg/min. Again the sample showed a weight increase from 419.43 ˚C to 0.056 mg/min. The weight put on and weight reduction showed that the $La_2In_{1.5}Al_{0.5}O_9$powder displayed simple reversible absorption - desorption of oxygen from the air. Fig 4.2 demonstrates the comparing DTA bend for the orchestrated powders. The examples arranged by this strategy with aspartic acid, endothermic and exothermic pinnacles are seen in the DTA bend.

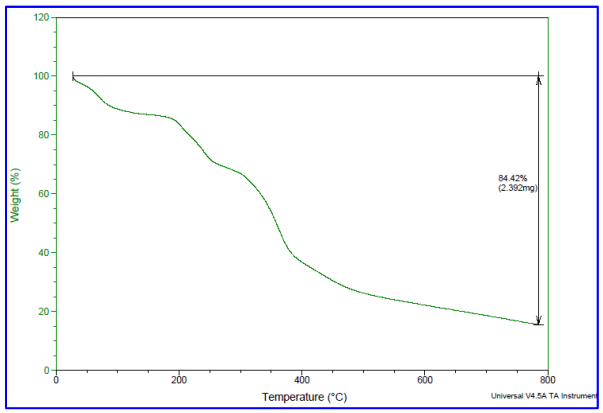

Fig. 4.2. TGA &DTA of $La_2In_{1.5}Al_{0.5}O_9$

4.3 FTIR Analysis Thinks About

FTIR spectroscopy was utilized to affirm the utilitarian gatherings display in the precious stone and is researched their vibrational conduct in the strong condition of $La_2In_{1.5}Al_{0.5}O_9$powder. It was recorded in the range of 4000 cm^{-1} to 400 cm^{-1}. The infrared spectrums of synthesized samples of $La_2In_{1.5}Al_{0.5}O_9$powder are shown in fig 4.3.

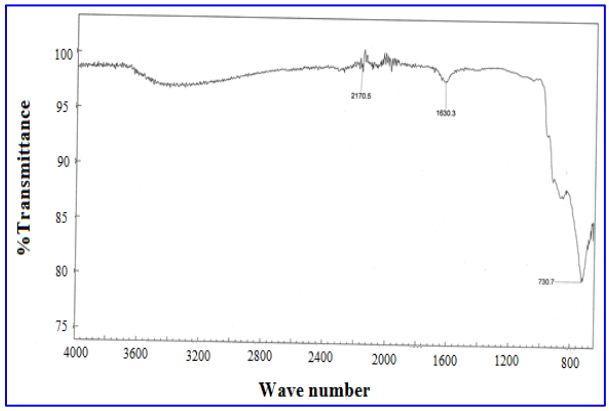

Fig. 4.3. FT-IR spectrum of $La_2In_{1.5}Al_{0.5}O_9$

The broadband at 1630.3 cm^{-1} can be assigned to the vibration mode of chemically bonded hydroxyl groups. The powder exhibited a strong bond at 600-800 cm^{-1} due to the stretching mode of the Indium -O bond in the structure. The peak that appeared at 730.3 cm^{-1} corresponds to the H-O-H bond mode confirming the presence of moisture in the sample. The peak that appeared at 2170.5 cm $^{-1}$ is due to the presence of CO_2 in the sample. The sample of $La_2In_{1.5}Al_{0.5}O_9$ exhibited a low-intensity peak at 730.3 cm $^{-1}$. The peak that appeared at 1630.3 cm^{-1} is related to the O-H stretching vibration of H_2O in the sample. The broadband at 1630.3 cm^{-1} can be assigned to the vibration mode of chemically bonded hydroxyl groups.

4.4 Scanning Electron Microscopy Studies

The surface morphology and size of the particles of $La_2In_{1.5}Al_{0.5}O_9$are appeared in fig 4.4. This material was set up by helped burning technique by utilizing aspartic acid demonstrated a wipe perspective and the particles connected together in agglomerates of various size and shapes (Gosh et al. 2005). The misfortune and permeable structure of these materials can be ascribed to a huge gas advancement amid the ignition response. Be that as it may, the structure remained exceedingly permeable, which took after the average structure for SOFC. However, indium doping essentially enhances brain development. The normal crystallite estimate was 28 nm. The particles are consistently dispersed.

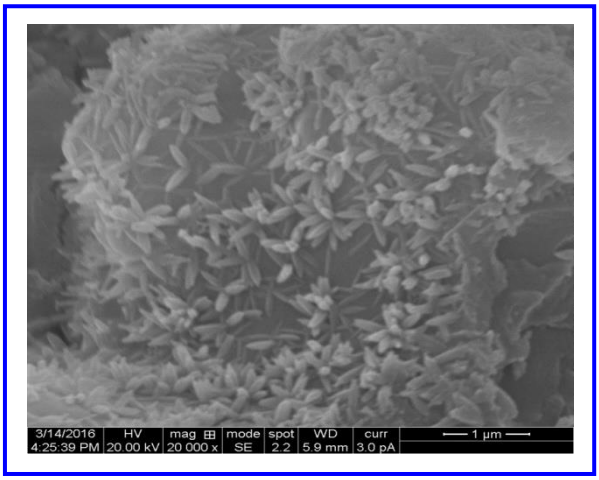

Fig. 4.4: SEM photograph of $La_2In_{1.5}Al_{0.5}O_9$

4.5 HRTEM Studies

The morphology and size of particles of $Nd_2Mo_{2-x}In_xO_9$ were observed by HRTEM micrograph are shown in fig 4.5. The ultra-fine particles were accomplished by helped ignition strategy. Because of the system, the ion measure was decreased, and the

agglomerates shaping were constrained (Bansal and Zhong, 2006). HRTEM micrograph recorded in brilliant field mode on the $Nd_2Mo_{1.5}In_{0.5}O_9$ powder showed the nearness of smaller nanocrystalline particles, and its ion was 25 nm. This ion measure is in great concurrence with these obtained from X – beam diffraction information.

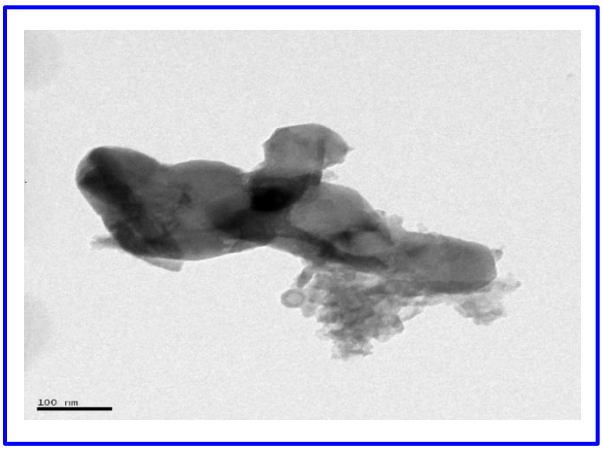

Fig 4.5: Transmission electron micrograph of $La_2In_{1.5}Al_{0.5}O_9$

4.6 Conductivity Studies

The Arrhenius plot of conductivity of the $La_2In_{2-x}Al_xO_9$ samples is shown in Fig 4.6. For pure $La_2In_2O_9$, a dramatic change of conductivity occurs at around 569 ˚C due to a phase transition. The Aluminum (Al) doped for Indium in $La_2In_{2-x}Al_xO_9$ tests show marginally enhanced conductivity at lower and higher temperatures. By and large, the higher unit-cell free volume in the oxide particle conductor is simpler for the oxygen-particle dispersion.

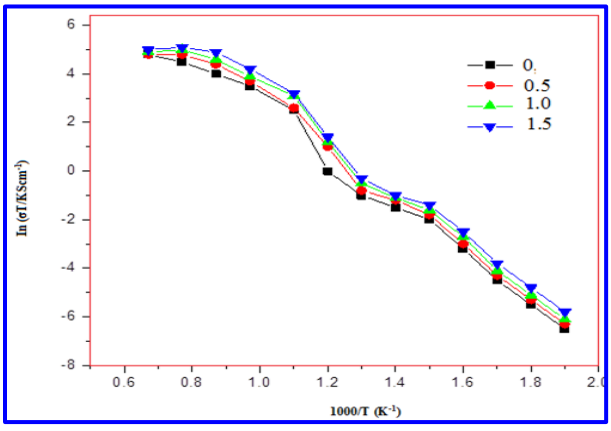

Fig 4.6: Arrhenius plot for the conductivity of $La_2In_{2-x}Al_xO_9$sample

In this way, the substitution of indium extraordinarily builds the free volume, and along these lines, the ionic conductivity of indium - doped samples likewise increments astoundingly. It can likewise be seen that sharp conduction increments up to x=0.5 in. The $La_2In_{1.5}Al_{0.5}O_9$sample exhibits the conductivity of 0.168 Scm^{-1} at 800 ˚C, compared with 0.160 Scm^{-1} for the undoped$La_2In_2O_9$. This result confirms that Aluminum (Al) - doping can improve the oxide ion conductivity of $La_2In_{2-x}Al_xO_9$at low and high temperatures. In addition, the high immaculateness and stage homogeneity of the present specimen could enhance the conductivity of Indium (Al) - doped $La_2In_{2-x}Al_xO_9$ samples (Berger et al. 2007).

5. CONCLUSION

The present investigation was carried out to improve the performance of $La_2In_{2-x}Al_xO_9$ by the synthesis method. The electrochemical behaviour of $La_2In_{2-x}Al_xO_9$based materials depends on the method of synthesis and sintering temperature. The present work was mainly focused on synthesis and ionic conductivity $La_2In_{2-x}Al_xO_9$.

REFERENCES

Bansal, N. P. and Zhong, Z., Combustion synthesis of $Sm_{0.5}Sr_{0.5}CoO_{3-x}$ and $La_{0.6}Sr_{0.4}CoO_{3-x}$ nanopowders for solid oxide fuel cell cathodes, *J. Fuel Sources*, 158(1), 148–153(2006). doi:10.1016/j.jpowsour.2005.09.057

Berger, D., Matei, C., Papa, F., Macovei, D., Fruth, V. and Deloume, J. P., Pure and doped lanthanum manganites obtained by combustion method, *J. Eur. Ceram. Soc.*, 27 4395–4398(2007). doi:10.1016/j.jeurceramsoc.2007.02.164

Cullity, B. D., Elements of X-ray Diffraction, Second Edition, Addision Wiley, New York (1978).

Garcia, R. and Hirata, G. A., New combustion synthesis technique for the production of $(In_xGa_{1-x})_2O_3$ powders: Hydrazine/metal nitrate method, *J. Mater. Res.*, Vol. 16(4), 1059-1065(2001) .

Ghosh, A., Sahu, A. K., Gulnar, A. K. and Suri, A. K., Synthesis and characterization of lanthanum strontium manganite, *Scr. Mater*., 52(12), 1305–1309(2005). doi:10.1016/j.scriptamat.2005.02.020

Jain, S. R. Adiga, K. C. and Pai Verneker, V. R., A new approach to thermochemical calculations of condensed fuel-oxidizer mixtures, *Combust. Flame*, 40, 71-79(1981). doi:10.1016/0010-2180(81)90111-5

Kostogloudis, G. Ch., Vasilakos, N. and Ftikos, Ch., Preparation and characterization of $Pr_{1-x}Sr_xMnO_{3\pm\delta}$ (x = 0, 0.15, 0.3, 0.4, 0.5) as a potential SOFC cathode material operating at intermediate temperatures (500–700 °C), *J. Euro Ceram Soc.*, 17(12), 1513-1521(1997). doi:10.1016/S0955-2219(97)00038-1

Lopez, O.A., Mckrittrick, J. and Shea, L. E., Fluorescence properties of polycrystalline Tm^{3+}-activated $Y_3Al_5O_{12}$ and Tm^{3+}-Li^{+} co-activated $Y_3Al_5O_{12}$ in the visible and near IR ranges**,** *J. Luin*., 71(1), 01-11(1997). doi:10.1016/S0022-2313(96)00123-8

Rajasekhar, M., Kalaivani, N., Preparation and Characterization of Gd1-xSrxAlO3 Cathode for Solid Oxide Fuel Cell, J. Environ. Nanotechnol.,, 6(3), 64-67(2017) doi:10.13074/jent.2017.09.173269

Sundar Manoharan, S. and Patil, K. C., Combustion Synthesis of Metal Chromite Powders**,** *J. Amer. Ceram. Soc.*, 75(4), (1992)1012. doi:10.1111/j.1151-2916.1992.tb04177.x